Memorandum Vol. 6, No. 6 / June 2019 / Optica 821

Reverberant cavity photoacoustic imaging

M. D. Brown,* E. Z. Zhang, B. E. Treeby, P. C. Beard, and B. T. Cox

Department of Medical Physics and Biomedical Engineering, University College London, Gower Street, London WC1E 6BT, UK
**Corresponding author: michael.brown.13@ucl.ac.uk*

Received 18 April 2019; accepted 23 April 2019 (Doc. ID 365445); published 19 June 2019

The number of ultrasound detectors required to produce photoacoustic tomography images can be reduced significantly by fully enclosing the imaging target in an acoustically reverberant cavity and exploiting the multiple reflections. This is demonstrated experimentally.

https://doi.org/10.1364/OPTICA.6.000821

Photoacoustic tomography (PAT) is a molecular imaging modality that can image biological soft tissue to greater depths than optical microscopy and with higher resolution than techniques that exploit diffuse light [1,2]. In PAT, the absorption of nanosecond pulses of light within the tissue results in acoustic transients that are detected at the tissue surface by an array of ultrasound detectors. These measurements can be used to reconstruct an image of the initial acoustic pressure distribution, which is a function of the inherent tissue absorption. In a conventional photoacoustic imaging system, the image resolution depends on several factors, including the detector bandwidth and the degree to which the array surrounds the target and therefore captures the emitted acoustic wavefront. Furthermore, the need to satisfy the spatial Nyquist sampling criterion can result in a requirement for a large number of detectors. Such high-channel-count acquisition presents challenges in terms of cost and complexity of fabrication for a full matrix array or data acquisition speed for a scanned detector.

One way to reduce the channel count is to encode the information from the space domain, where it is costly to record, on to the time domain, where it is relatively inexpensive. This approach has been exploited in optical imaging, for example, with the serial time-encoded amplified microscopy (STEAM) camera [3] and the optofluidic microscope [4]. In photoacoustic imaging, initial steps along this road have been taken by using reflectors [5] and scatterers [6] to map the emitted acoustic wavefront onto the measured time-resolved signal in order to extend the effective array aperture without increasing the channel count. Using an alternative approach, it has been shown theoretically that the channel count can be dramatically reduced, even to one, by using a reverberant cavity [7]. With this method, forming an image with a few detectors or a single detector is possible because the additional information contained in the temporally extended reverberant field is equivalent to that contained in the field measured in the absence of a cavity at many spatial points. This equivalence means that, instead of recording the photoacoustic waves at many spatial points for a short time, measurements can be made at just a few points but for a longer time, offering a significant reduction in the cost and complexity of the imaging system. Here, this concept is demonstrated experimentally for the first time.

A schematic of the experimental setup is shown in Fig. 1. A water-filled cuboid reservoir, ~18 × 20 × 20 mm, was constructed from BK7 glass. A Q-switched Nd:YAG laser ($\lambda = 1064$ nm, 50 mJ, 8 ns) was used for PA excitation, and a highly sensitive micro-resonator fiber-optic ultrasound sensor that exhibits a near omnidirectional response was used for detection [8]. A 2D geometry was chosen to demonstrate the principle, so vertical cylindrical absorbers were used as imaging targets.

In order to acquire an image, the fiber-optic sensor is scanned along a line as shown in Fig. 1. The acoustic pressure time series measured by the fiber-optic sensor at detector position (x_d, y_d) can be written as a linear combination of the impulse response functions between that point and every image point (x_s, y_s). [9] One approach to reconstructing an image of the initial pressure distribution p_0 is therefore to invert a matrix of impulse responses measured by placing physical point sources at every position. However, this is very labor intensive. Here, a different, model-based approach was taken. The cavity geometry was determined accurately using a one-off calibration measurement and model-based optimization. The derived cavity parameters were then used to construct an acoustic model of the cavity that could then be used to reconstruct the photoacoustic image using a method based on time reversal [5,10] The latter involves propagating the recorded acoustic time series $p_n(t)$ through the model in time-reversed order back to the initial time t0.

The calibration step is illustrated in Figs. 2(a) and 2(c). A single cylindrical absorber is illuminated, and the sensor is scanned along a line, acquiring PA signals at each point. Using this data, an active-set optimization algorithm was used to find accurate values for the cavity dimensions (d_x, d_y), the detector positions $\boldsymbol{r}_d = \{(x_d^n, y_d^n), n = 1, \ldots, N\}$, and sound speed c. The correct values were assumed to be those that maximized the reconstructed pressure at the location of the single absorber. To constrain the optimization, limits were set on the parameters (d_x, d_y, c) based on estimated ranges for their possible values (e.g., the sound speed will likely fall between 1460–1520 m/s). Also, it was known that

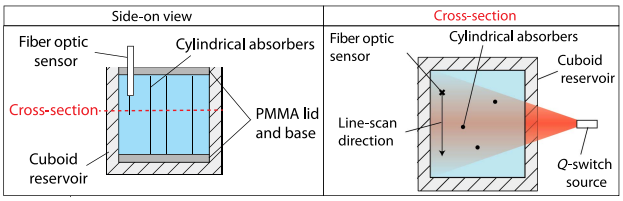

Fig. 1. Schematic of experimental setup.

the detector positions $\boldsymbol{r}_d$ lay along a line with a fixed, known spacing dr between points, so $\boldsymbol{r}_d = \{(x_0 + n \cdot dr \cdot \cos\theta, y_0 + n \cdot dr \cdot \cos\theta), n = 1, \ldots, N\}$ with x_0, y_0, and θ being the unknowns.

To demonstrate the concept, the following experiment was performed. First, a single absorbing synthetic hair was placed in the cavity [Fig. 2(a)] and used to calibrate the cavity parameters as described above. Then, once the calibration step had been completed, the system was then used to image a target comprising seven synthetic hairs [Fig. 2(b)]. The time series of the reverberant signals generated from the imaging target were recorded separately at 15 detector positions spaced by 300 μm. In practice these positions could be anywhere, but optimally they would coincide with the maxima of the cavity modes [7,9].

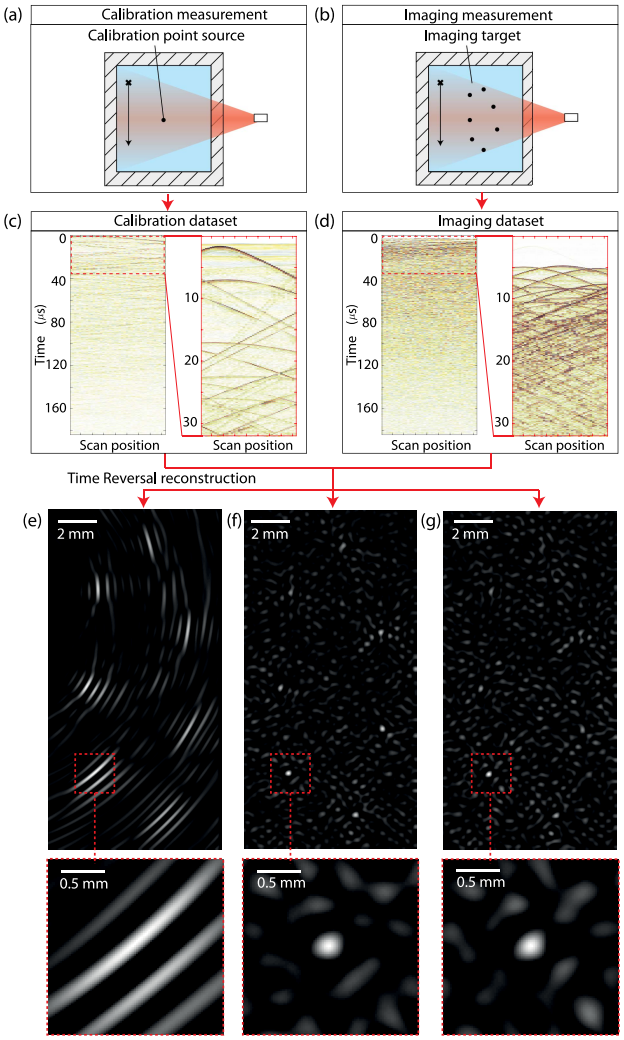

Fig. 2. Reconstruction approach and reconstructed images. Two separate measurements are made of (a) a single-point calibration source and (b) the imaging target. (c) The calibration time series are fitted to a model to obtain the cavity dimensions. (d) The imaging time series are used to form photoacoustic images. (e) Photoacoustic image generated without taking into account the multiple reflections. (f) Image reconstructed from the first 60 μs of the data. (g) Image from the first 280 μs.

Three different reconstructions were performed to demonstrate the effect of the reverberant signals on the reconstructed image as shown in Figs. 2(e)–2(g). The image in Fig. 2(e) was reconstructed assuming free-field conditions, i.e., the model used for the time-reversal reconstruction did not include reflections and is therefore the image that would have been obtained using a conventional, non-reverberant imaging approach. In Figs. 2(f) and 2(g), however, the reverberant signal was included, with time records of 60 μs and 280 μs, respectively. It is clear from these reconstructions that the image spatial resolution and fidelity can be very significantly improved by exploiting the multiple reflections inside the cavity. The artefacts resulting from the limited view of the detection aperture visible in Fig. 2(e) are significantly reduced in Fig. 2(f), in which each of the seven hairs is clearly resolved.

The image quality initially improves as a function of the length of the time series used in the reconstruction, as the reflections contribute beneficially to the image, but eventually the quality decreases. This is because small inaccuracies in the cavity dimensions are compounded over time resulting in misalignments in the wavefronts associated with later reflections. In other words, the later arriving signals are increasingly mismatched to the model. This is illustrated by Fig. 2(g), which was generated using 280 μs of data and consequently exhibits a higher level of background noise than Fig. 2(f), which was generated from 60 μs of data. A disadvantage of this approach is therefore that the image quality is strongly affected by uncertainty in the calibration step, e.g., here, an error of 10 μm in d_x generates an error of ∼140 μm after 200 μs.

This paper has shown that a reverberant cavity can be used to achieve good image quality with a greatly reduced channel count (>8× compared to full view detection). By mapping the information about the initial acoustic pressure distribution onto reverberant signals recorded on just a few channels, this technique could be used to create low-cost photoacoustic imaging systems for studying targets that can be partially or fully enclosed, including small animals such as zebrafish or *ex vivo* tissue samples.

Funding. Biotechnology and Biological Sciences Research Council (BBSRC) (174569); H2020 European Research Council (ERC) Advanced Grant (741149).

REFERENCES

1. P. Beard, Interface Focus. **1**, 602 (2011).
2. M. Xu and L. V. Wang, Rev. Sci. Instrum. **77**, 041101 (2006).
3. K. Goda, K. K. Tsia, and B. Jalali, Nature **458**, 1145 (2009).
4. Y. Zhao, Z. Stratton, F. Guo, M. Lapsley, C. Chan, S. Lin, and T. Huang, Lab Chip **13**, 17 (2013).
5. R. Ellwood, E. Zhang, P. Beard, and B. Cox, J. Biomed. Opt. **19**, 126012 (2014).
6. X. Deán-Ben, A. Özbek, and D. Razansky, Proc. SPIE **10878**, 108781K (2019).
7. B. Cox and P. Beard, J. Acoust. Soc. Am. **125**, 1426 (2009).
8. J. Guggenheim, J. Li, T. Allen, R. Colchester, S. Noimark, O. Ogunlade, I. Parkin, I. Papakonstantinou, A. Desjardins, E. Zhang, and P. Beard, Nat. Photonics **11**, 714 (2017).
9. A. Derode, A. Tourin, and M. Fink, J. Appl. Phys. **85**, 6343 (1999).
10. B. Treeby and B. Cox, J. Biomed. Opt. **15**, 021314 (2010).